TÜBİTAK

Turkish Journal of Medical Sciences

http://journals.tubitak.gov.tr/medical/

Research Article

Turk J Med Sci
(2016) 46: 572-581

doi:10.3906/sag-1501-173

Role of FLT3 in the proliferation and aggressiveness of hepatocellular carcinoma

Muammer Merve AYDIN[1], Nermin Sumru BAYIN[1], Tolga ACUN[2], Mustafa Cengiz YAKICIER[3], Kamil Can AKÇALI[4,*]

[1]Department of Molecular Biology and Genetics, Bilkent University, Ankara, Turkey
[2]Department of Molecular Biology and Genetics, Faculty of Sciences and Arts, Bülent Ecevit University, Zonguldak, Turkey
[3]Department of Molecular Biology and Genetics, Acıbadem University, İstanbul, Turkey
[4]Department of Biophysics, Ankara University, Faculty of Medicine, Ankara, Turkey

Received: 01.02.2015 • **Accepted/Published Online:** 26.05.2015 • **Final Version:** 17.02.2016

Background/aim: Previously we showed that Fms-like tyrosine kinase (FLT3) changes its cellular localization upon partial hepatectomy, suggesting a role in liver regeneration. FLT3 was also shown to play an important function in cellular proliferation and activation of PI3K and Ras. Thus, we aimed to investigate the role of FLT3 in hepatocellular tumorigenesis utilizing in vitro and in vivo models.

Materials and methods: We used Snu398 cells that express FLT3. We investigated these cells' in vitro proliferation and invasion abilities by treatment with the FLT3 inhibitor K-252a or by knocking-down with FLT3 shRNA,. Furthermore, the effect of blocking FLT3 activity and expression during in vivo tumorigenesis was assessed with xenograft models.

Results: After K-252a treatment or stable knock-down, these cells' proliferation and migration abilities were highly diminished in vitro. In addition, significant diminution in tumorigenicity of Snu398 cells was also obtained in vivo. When FLT3 knocked-down Snu398 cells were injected into nude mice, we did not detect αSMA expression in these tumors, suggesting a role for FLT3 in in vivo invasiveness.

Conclusion: Our data provided evidence that FLT3 has a crucial role both in hepatocarcinogenesis and its invasiveness. Therefore, targeting FLT3 and/or its activity may be a promising tool for combating hepatocellular carcinomas.

Key words: Fms-like tyrosine kinase, liver cancer, regeneration, invasiveness, tyrosine kinase

1. Introduction

Hepatocellular carcinoma (HCC) is the sixth most common neoplasm worldwide (1) and the third leading cause of cancer-induced death following lung and stomach cancers due to the lack of targeted therapies and resistance to chemotherapeutic agents (2). There is strong evidence that shows a link between the disease and risk factors such as HBV, HCV infection, aflatoxins, and excessive alcohol consumption (3).

Fms-like tyrosine kinase (FLT3) is a type III receptor tyrosine kinase (RTK) and a hematopoietic lineage marker (4). FLT3 signaling was shown to play an important role in the stimulation of myeloid and lymphoid progenitor cell proliferation (4). Signaling molecules such as PI3K and Ras were activated when FLT3 bound to FLT3 ligand (FLT3L) (5). Upon ligand binding, FLT3 changes conformation and forms a homodimer, which brings the kinase domains in close proximity for phosphorylation. After dimerization, downstream signaling is initiated, followed by internalization and subsequent degradation of the complex. These processes happen very quickly where the first degraded products of the FLT3L-FLT3 complex are seen within 20 min after stimulation (6).

FLT3 signaling pathways participate in many physiological processes throughout embryogenesis and development. FLT3 is crucial for hematopoietic cell development, and aberrancy in the functioning of FLT3 was demonstrated to cause different leukemia types (7). In addition to its role in stimulating myeloid and lymphoid progenitor cell proliferation and as an indicator of hematopoietic lineage, FLT3 is also a marker of hepatic bipotential progenitor cells or oval cells in rodents (8,9). We previously demonstrated that FLT3 is activated during liver regeneration in rats, suggesting that FLT3 may contribute to the proliferation of hepatocytes (10). Since the fetal liver is the primary site for hematopoiesis during early development, a close relationship between the hematopoietic cells and the hepatic parenchyma can easily be drawn (11). Signals between the hematopoietic cells within the fetal liver and the hepatocytes are crucial for the

* Correspondence: akcali@ankara.edu.tr

development of both cell types. Oncostatin M secreted from hematopoietic cells induces hepatocyte differentiation via increased HNF4α expression, and the coculture of fetal hepatocytes with hematopoietic cells showed increased growth and proliferation of hematopoietic cells (12).

Since FLT3 participates in liver regeneration (10) and cellular proliferation (13,14), and there is a close relationship between fetal liver and hematopoiesis (15,16), we hypothesized that FLT3 may have a role in hepatocellular tumorigenesis and the FLT3 expressing HCC line would be an appropriate tool to test its role. We tested our idea with both in vitro and in vivo models after knocking down FLT3 with specific shRNA or using the specific kinase inhibitor K-252a.

2. Materials and methods

2.1. Cell culture

Huh7, Hep40, and SK-Hep-1 cells were cultured in DMEM (HyClone, USA) supplemented with 10% FBS and 100 U/mL penicillin-streptomycin. Snu398 cells were cultured in RPMI1640 (HyClone) supplemented with 10% FBS, 100 U/mL penicillin-streptomycin, and 0.1 mM nonessential amino acids (HyClone). Cells were incubated at 37 °C with 5% CO_2 and media were changed every 3 days.

2.2. K-252a treatment of Snu398 cells

K-252a kinase inhibitor (Nocardiopsis sp.) (Calbiochem, USA) was used at a final concentration of 200 nM 2 h prior to experiments, as we used it in our previous studies (17). The same volume of DMSO was used as a control.

2.3. Stable knock-down of FLT3 mRNA in Snu398 cells

FLT3 shRNA (Openbiosystems, USA) and GFP (Clontech Laboratories, USA) plasmids were transfected using X-tremeGENE HP DNA transfection reagent (Roche Applied Science, Germany). Snu398 cells were seeded on 6-well plates the day before transfection. First 1 μg of plasmid, either shRNA containing or not, was used for each well together with the X-tremeGENE HP DNA transfection reagent. Before transfection, the X-tremeGENE HP DNA transfection reagent and plasmid DNA were equilibrated to 15 to 25 °C. FLT3 shRNA and GFP plasmids were diluted to 1 μg plasmid DNA/100 μL medium (0.01 μg/μL) at a 1:3 ratio using serum-free RPMI. Next, 2 μL of X-tremeGENE HP DNA transfection reagent was added into each 100 μL of plasmid DNA diluent and incubated at room temperature for 15 min. Following incubation, the mixture was added dropwise on the top of the cells and left in the incubator for 48 h. The FLT3 mRNA expression of the transfected cells was analyzed by performing RT-PCR using half of the cells in each well. Upon observing a decrease in the FLT3 expression in shRNA transfected, but not in empty vector transfected cells, all cells that underwent transfection were plated into two 75-cm^2 flasks separately in fresh RPMI containing puromycin (Sigma-Aldrich, USA) with 0.75 μg/mL final concentration. After 2 weeks, cells were harvested and diluted in puromycin containing RPMI to seed one cell per each well of a 96-well plate. In 2 to 3 weeks, plasmid containing cells were expected to form colonies that either had decreased or unchanged expression of FLT3.

2.4. Total RNA isolation and reverse transcription

Cells were trypsinized and total cellular RNA was isolated from the precipitate by using the RNeasy mini kit (Qiagen, Germany) according to the manufacturer's protocol, with additional DNase treatment. The cDNAs were synthesized from the total RNA samples with the DyNAmo cDNA synthesis kit (Finnzymes, Finland) according to the manufacturer's protocol. cDNA amplification for *flt3* and *gapdh* was performed by using DyNAzyme II (Finnzymes) with the following primers: human FLT3: Forward 5'GGAAGAAGAGGAGGACTTA3', Reverse 5'AGGTCTCTGTGAACACACGA3'; human GAPDH: Forward 5'GGCTGAGAACGGGAAGCTTGTCAT3'; Reverse 5'CAGCCTTCTCCATGGTGGTGAAGA3'. The initial denaturation step was at 95 °C for 5 min, followed by 30 cycles for *flt3* and 23 cycles for *gapdh* of denaturation for 30 s at 94 °C, annealing for 30 s at 60 °C, followed by extension for 30 s at 72 °C. A final extension at 72 °C for 5 min was applied to all reactions.

2.5. Total protein isolation and Western blotting

Cells were scraped and the precipitate was treated with a lysis buffer containing 0.05 M Tris-HCl, 1X protease inhibitor, 0.25 M NaCl, and 1% (v/v) IGEPAL. Protein concentration was determined with Bradford protein assay (18). First 20 μg of the total protein was separated on 10% SDS-PAGE and transferred to a polyvinylidene fluoride membrane. After the membrane was blocked for 2 h at room temperature, FLT3 and Calnexin primary antibodies (1:1000) were applied overnight at 4 °C. Anti-rabbit-HRP (1:1000) was applied for 1 h. Finally, Super Signal West Femto maximum sensitivity substrate (Thermo Scientific, USA) was used. All antibodies were purchased from Santa Cruz (Santa Cruz Biotechnology Inc., USA).

2.6. Immunofluorescence staining for Snu398 cells

Cells were grown on coverslips and following methanol fixation, blocking was performed at room temperature for 1 h. Anti-FLT3 antibody (Santa Cruz; 1:200) incubation was done at room temperature for 1 h. Alexa Fluor 568-tagged anti-rabbit IgG secondary antibody (Invitrogen, USA) (1:1000) was used for another 1 h at room temperature. Coverslips were mounted with UltraCruz mounting medium with DAPI (Santa Cruz) for counter staining. Slides were observed with a fluorescent microscope (Leica TCS/SP5). The excitation wavelengths for Alexa Fluor 568 and DAPI were 578 nm and 359 nm, respectively.

2.7. Immunofluorescence staining for frozen sections

The primary antibody of FLT3 (Santa Cruz) and αSMA (Abcam) was applied to the cryo-sections (5 μm) of tumor xenografts at a 1:200 concentration for 1 h at room temperature. FITC-tagged anti-rabbit IgG secondary antibody (Sigma-Aldrich) (1:200) was used for 1 h at room temperature. Slides were mounted with UltraCruz mounting medium with DAPI (Santa Cruz) for counter staining and observed with a fluorescent microscope (Leica TCS/SP5). The excitation wavelengths for FITC and DAPI were 490 nm and 359 nm, respectively.

2.8. MTT assay

Cell proliferation Kit I (MTT) (Roche, Switzerland) was used to check the proliferation characteristics of Snu398 cells upon K-252a treatment or FLT3 shRNA transfection. Snu398 cells were either treated with K252-a or DMSO 2 h prior to the experiment. Next, 10^4 cells/well were seeded into a 96-well plate and left at 37 °C for 24 h. FLT3 shRNA and empty vector transfected Snu398 cells were seeded at a density of 5×10^3 cells/well and left at 37 °C for 72 h. Subsequent labeling and solubilization steps were performed according to the manufacturer's protocol. OD values at 551 nm were read with Synergy H1 microplate reader (BioTek Instruments Inc., USA).

2.9. Wound healing assay

After cells reached 100% confluency on the 6-well plates, 3 vertical scratches were made. Cells were then incubated either with 10% FBS or 2% FBS to induce serum starvation. Wounds were monitored for 48 h and photos of the same regions were taken in 24-h intervals. Healed wound distance was measured by calculating the average of the difference between the initial and final wound sizes of 10 separate areas.

2.10. Matrigel invasion assay

Matrigel Basement Membrane Matrix (BD Biosciences, USA) was diluted, put into a 24-well transwell plate (Corning Incorporated Life Sciences, USA), and incubated at 37 °C for 4–5 h. Then 10^5 cells were put into each of the Matrigel coated transwells. The lower chamber of each well was filled with RPMI containing 5 μg/mL fibronectin and left at 37 °C for 20–24 h. Invaded cells were stained with Diff-Quick staining solution kit (IMEB Inc., California, USA). Noninvaded cells were removed and the invaded cells were counted under a light microscope.

2.11. Nude mice tumor xenografts

Each group contained 5 male CD1 nude mice. First 6×10^6 cells and their controls were injected subcutaneously to the opposite sides of the animals. The animals were permitted unlimited access to food and water at all times and were housed under controlled environmental conditions (22 °C) with a 12 h light and 12 h dark cycle in the animal holding facility of the Department of Molecular Biology and Genetics at the Bilkent University. This study protocol complied with Bilkent University's Local Animal Ethic Committee (BILHADYEK) guidelines on humane care and use of laboratory animals according to the criteria outlined in European Convention ETS 123.

2.12. Statistical analysis

All data are expressed as means ± SD. Student's t-test and the Mann–Whitney U test were used with a significance level $P < 0.05$.

3. Results

3.1. Expression pattern of FLT3 in Snu398 cells

We examined the expression of FLT3 in four HCC lines. Amongst them, Huh7 and Hep40 are well differentiated (WD), while Snu398 and SK-Hep-1 are poorly differentiated (PD) HCC lines (19). FLT3 expression was observed in Snu398 cells, and to a lesser degree in Hep40 cells at the mRNA level (Figure 1A). However, this slight expression of FLT3 in Hep40 cells disappeared at the protein level, and only in Snu398 cells FLT3 protein expression was detectable (Figure 1B). Therefore, we decided to utilize the Snu398 HCC line for in vitro experiments to test our hypothesis. When we stably knocked-down FLT3 expression by using specific shRNA in Snu398 cells, FLT3 mRNA expression was decreased in these transfected cells (Snu398 FLT3-shRNA) when compared with that of empty vector transfected cells (Snu398 pGIPz) (Figure 1C). The decrease was approximately 45% (Figure 1D). In addition, when we performed immunofluorescence staining against FLT3 protein, we found that in contrast to abundant positive staining in empty vector transfected cells, few cells express FLT3 protein in FLT3 shRNA transfected cells (Figure 1E). In parallel to our RT-PCR data, the amount of FLT3 expression dropped almost 50% in Snu398 FLT3-shRNA transfected cells as compared with that of Snu398 pGIPz transfected cells (Figure 1F).

3.2. Functional analysis of FLT3 in Snu398 following inhibition with K-252a and knocking-down via shRNA transfection

In order to investigate the functional role of FLT3 in HCC, we analyzed in vitro proliferation, migration, and invasiveness abilities after treating with the FLT3 inhibitor K-252a or transfecting with a specific shRNA for FLT3 in Snu398 cells. Our MTT results showed that the proliferation ability of Snu398 cells diminished following K-252a treatment compared to DMSO treated cells (Figure 2A) and this decrease was statically significant ($P < 0.05$). Similarly there was a decrease in the proliferative capacity of Snu398 cells when FLT3 was knocked down, albeit not statistically significant (Figure 2B).

To assess the effect of FLT3 in the invasiveness of Snu398 cells (Figures 2C and 2D), following K-252a

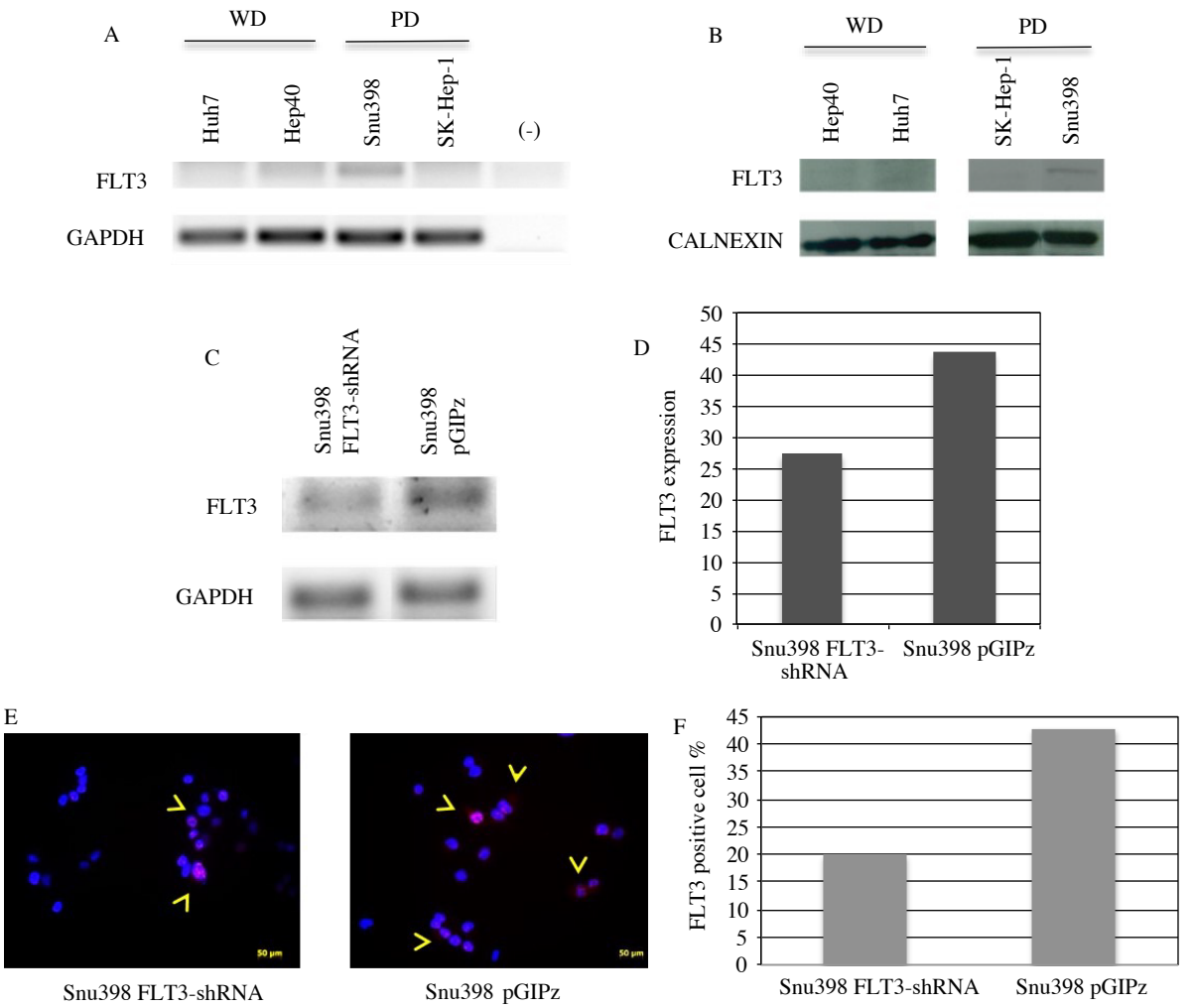

Figure 1. Expression of FLT3 in vitro. a). FLT3 expression in well differentiated (WD) and poorly differentiated (PD) HCC cell lines at the mRNA level. The mRNA levels are shown by RT-PCR; *gapdh* was used as a loading control; b) FLT3 expression in well differentiated (WD) and poorly differentiated (PD) HCC cell lines at the protein level. The protein levels are shown by Western blot; CALNEXIN was used as a loading control; c) expression of FLT3 mRNA in Snu398 cells transfected with shRNA against FLT3 (Snu398 FLT3-shRNA) and in empty vector transfected cells (Snu398 pGIPz); *gapdh* was used as a loading control; d) quantitation of the expression of FLT3 mRNA after transfection; e) Alexa Fluor 568 labeled FLT3 protein expression in FLT3 shRNA transfected (Snu398 FLT3-shRNA) and empty vector transfected cells (Snu398 pGIPz); nuclei were stained with DAPI; f) the percentage of the FLT3 protein expression was calculated by dividing FLT3 positive cells by the total number of cells based on their DAPI staining both in FLT3 shRNA transfected (Snu398 FLT3-shRNA) and empty vector transfected cells (Snu398 pGIPz).

treatment for 2 h (Figure 2C, blue lines), we observed a diminution in the wound healing capacity of Snu398 cells as compared with that of DMSO treated cells (Figure 2C, red lines). We also found a similar result after transfecting the cells with FLT3 specific shRNA (Figure 2D). FLT3 knocked-down cells' wound healing capacity (Figure 2D, blue lines) decreased as compared with that of empty vector transfected control cells (Figure 2D, red lines). We also performed a Matrigel invasion assay and compared the number of invaded colonies (Figure 2E). Our results showed that the invasiveness of Snu398 cells decreased significantly after they were treated with inhibitor K-252a or transfected with FLT3 shRNA ($P < 0.05$).

3.3. Role of FLT3 in the tumorigenicity and the invasiveness of Snu398 cells in vivo

Snu398 cells were either treated with K-252a or stably transfected by FLT3 shRNA prior to injection into the nude mice for in vivo studies. Tumor size decreased considerably when Snu398 cells were transplanted after K-252a treatment (Figures 3A–3C) and FLT3 shRNA

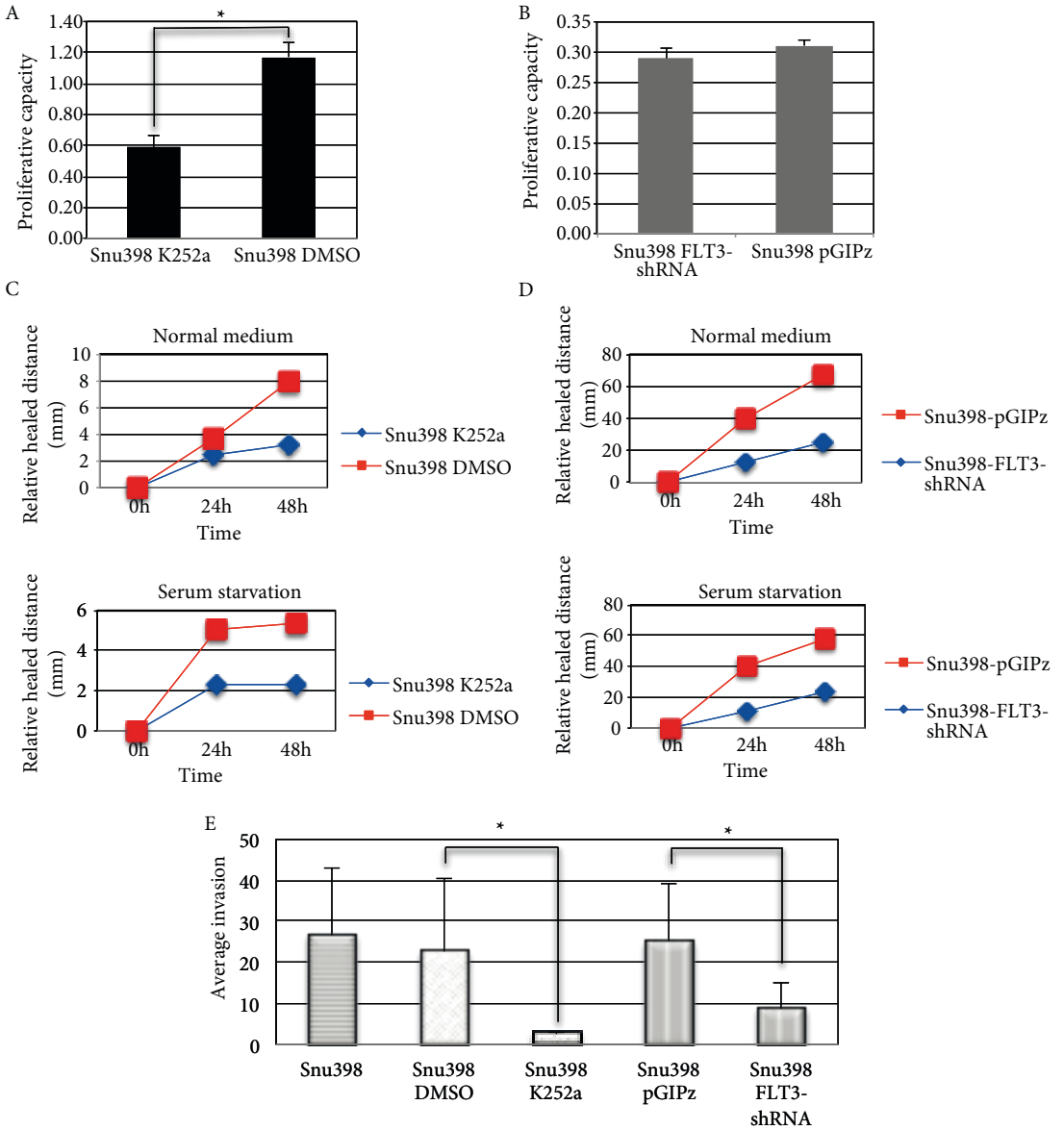

Figure 2. Effects of FLT3 on the in vitro proliferation, migration, and invasion ability of Snu398 cells. a) Proliferation ability of Snu398 cells after 2 h of K-252a and DMSO treatment (*: $P < 0.05$) by MTT assay; b) proliferation ability of Snu398 cells after transfecting with FLT3 specific shRNA (Snu398 FLT3-shRNA) and empty vector (Snu398 pGIPz) by MTT assay; c) quantification of the effects of K-252a treatment (blue lines) as compared with DMSO treatment (red lines) on the wound healing capacity of Snu398 cells in normal and serum starved media; d) quantification of the effects of FLT3 specific shRNA transfected Snu398 cells (Snu398 FLT3-shRNA; blue lines) and empty vector transfected cells (Snu398 pGIPz; red lines) on the wound healing capacity of Snu398 cells in normal and serum starved media. The effects of FLT3 on the in vitro invasion of Snu398 cells are shown by the Matrigel assay; e) quantification of the number of invaded colonies of Snu398 cells grown in normal medium (Snu398), control medium (Snu398 DMSO), with an inhibitor (Snu398 K-252a), following empty vector transfection (Snu398 pGIPz) and specific FLT3 shRNA transfection (Snu398 FLT3-shRNA) (*: $P < 0.05$).

transfection (Figures 3D–3F) as compared with the tumor size of the controls. Differences in the average tumor volumes of xenografts injected with Snu398 cells in the presence or absence of the inhibitor were statistically significant ($P < 0.05$) (Figure 3C). Snu398 cells that were treated with the FLT3 inhibitor (Snu398 K-252a) did not form any measurable tumor in the area shown by the red arrow, whereas Snu398 cells that were treated with DMSO as a control (Snu398 DMSO) formed tumor masses in the area shown by the blue arrow (Figure 3A). On the

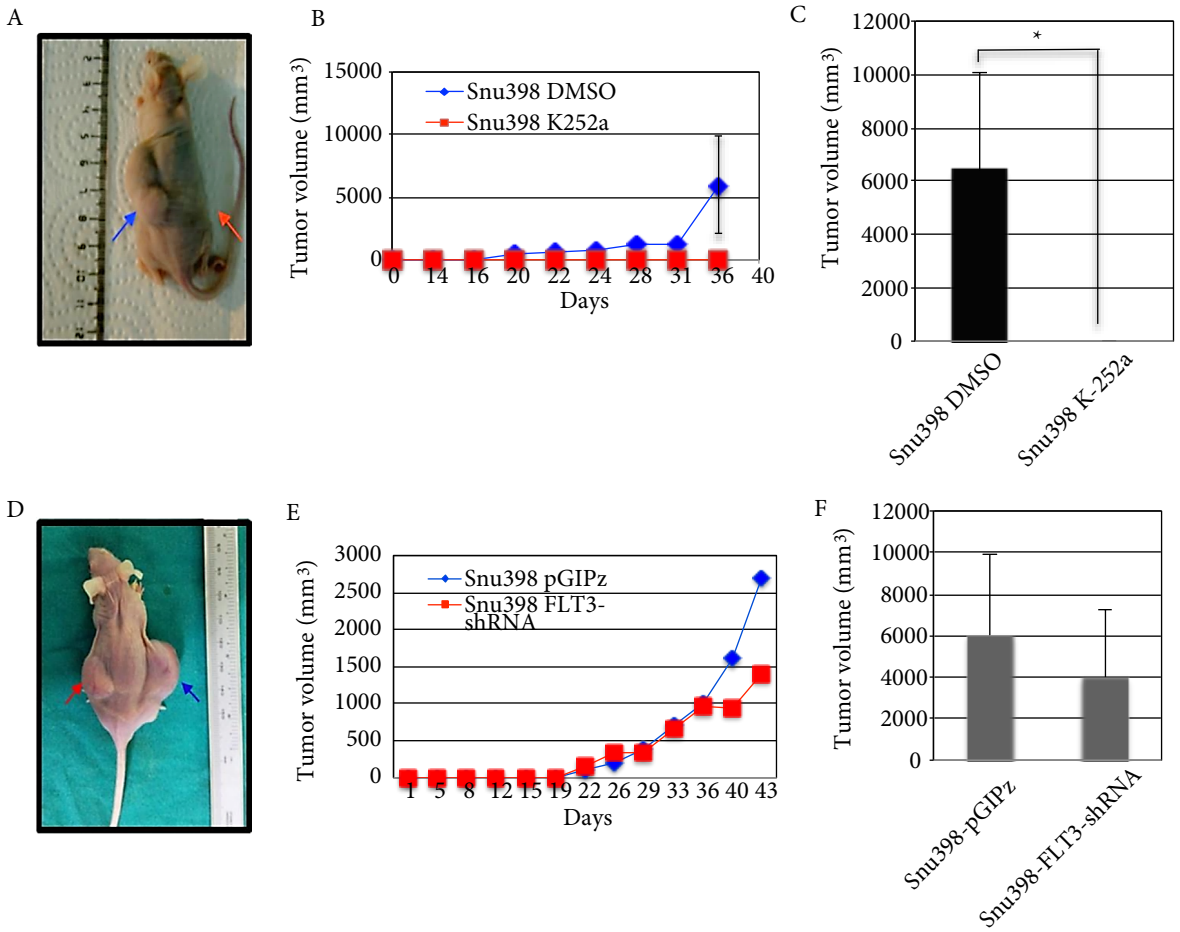

Figure 3. Effects of FLT3 on the in vivo tumorigenicity of Snu398 cells. a) A representative photograph of a mouse injected with FLT3 inhibitor treated Snu398 cells (Snu398 K-252a) or with DMSO treated Snu398 cells as a control (Snu398 DMSO). Injection sites are shown by the red and blue arrows, respectively; b) tumor growth curve of the K252-a and DMSO treated Snu398 cells; c) the differences in the average tumor volumes of xenografts injected with Snu398 cells in the presence or absence of an inhibitor were statistically significant (*: $P < 0.05$); d) a representative photograph of a mouse injected with FLT3 specific shRNA transfected Snu398 cells (Snu398-FLT3-shRNA) or with empty vector transfected Snu398 cells (Snu398-pGIPz). Injection sites are shown by red and blue arrows, respectively; e) tumor growth curve of FLT3 shRNA and empty vector (pGIPz) transfected Snu398 cells; f) the differences in the average tumor volumes of xenografts generated by FLT3 shRNA and control transfected Snu398 cells were not statistically significant.

other hand, the average size of the tumor formed after injecting FLT3 shRNA transfected Snu398 (Snu398-FLT3-shRNA) cells was 33% less than that of the empty vector transfected Snu398 (Snu398-pGIPz) cells (Figure 3F), but the difference was not statistically significant.

In addition, we examined the expression of FLT3 and αSMA as markers for invasiveness in the xenografts with immunofluorescence staining. We observed that very few cells express the FLT3 protein in the tumor sections that were generated with FLT3 shRNA transfected Snu398 (Snu398-FLT3-shRNA) when compared with the sections of empty vector transfected Snu398 (Snu398-pGIPz) cells (Figures 4A and 4B). When we quantitated the percentage of FLT3 positive cells, we found that only 10% of the cells express the FLT3 protein in the tumors that were generated with FLT3 shRNA transfected Snu398 (Snu398-FLT3-shRNA) cells. On the other hand, this rate increased to 68% in the tumors that were generated with empty vector transfected Snu398 (Snu398-pGIPz) cells (Figure 4C). By comparing the expression of αSMA, we also explored whether the reduction in the tumor size reflects the less invasive nature of FLT3 shRNA transfected Snu398 cells. Our results showed that when FLT3 expression was knocked down, few cells expressed αSMA (Figure 4D). However, when the cells were transfected with the empty vector, we detected abundant αSMA protein expression in the tumor sections as shown by the red arrowheads (Figure 4E). αSMA expression was seen in 25% of the cells in the FLT3 shRNA transfected Snu398 xenograft, whereas it was 58% in the empty vector transfected Snu398 xenograft (Figure 4F).

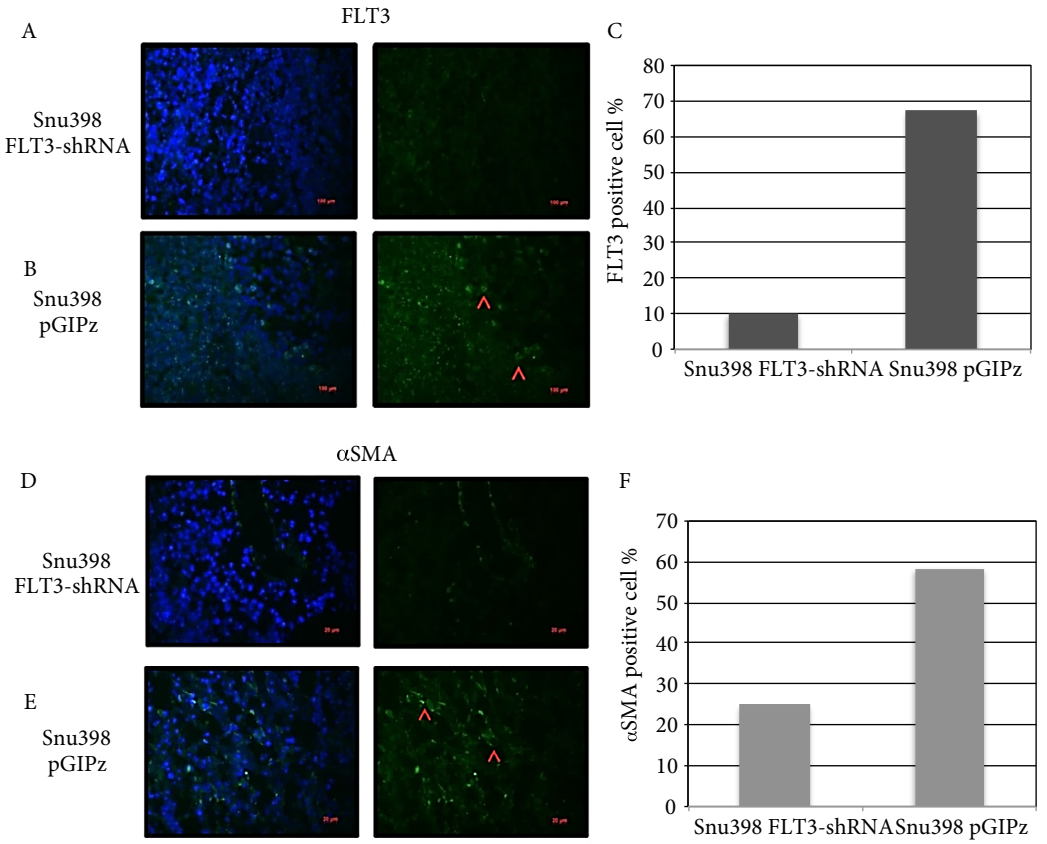

Figure 4. Effects of FLT3 on the invasiveness of Snu398 cells in vivo. a) Expression of FITC labeled FLT3 protein in the section of the tumor in nude mice generated by Snu398 cells transfected with FLT3 shRNA; merged pictures of the sections with DAPI stained nuclei are shown on the left panel of the sections and red arrowheads denote FITC labeled FLT3 positive cells; b) expression of FITC labeled FLT3 protein in the section of the tumor in nude mice generated by Snu398 cells transfected with pGIPz; merged pictures of the sections with DAPI stained nuclei are shown on the left panel of the sections and red arrowheads denote FITC labeled FLT3 positive cells; c) quantification of FLT3 positive cells with ImageJ; d) expression of FITC labeled αSMA protein in the section of the tumor in nude mice generated by Snu398 cells transfected with FLT3 shRNA; merged pictures of the sections with DAPI stained nuclei are shown on the left panel of the sections and red arrowheads denote FITC labeled αSMA positive cells; e) expression of FITC labeled αSMA protein in the section of the tumor in nude mice generated by Snu398 cells transfected with pGIPz; merged pictures of the sections with DAPI stained nuclei are shown on the left panel of the sections and red arrowheads denote FITC labeled αSMA positive cells; f) quantification of αSMA positive cells with ImageJ.

4. Discussion

Treatment of HCC remains an urgent health concern and there is a growing need for new therapeutic candidates. In this study, we aimed to find a novel potential biomarker for HCC and focused on FLT3. FLT3 is not only a marker for hematopoietic lineage, but also a marker for hepatic oval cells that differentiate into hepatocyte and bile duct lineages (20,21). In addition, a close relationship between liver development and hematopoiesis also implies that FLT3 signaling may have a critical function in the liver (22,23). Furthermore, we have previously shown that FLT3 may play a role in liver regeneration (10).

We analyzed the expression level of FLT3 in four HCC cell lines. We found FLT3 protein expression only in Snu398, a poorly differentiated (PD) HCC line (19). Differentiation is used in tumor grading systems and PD cancers tend to grow and spread faster than well differentiated or undifferentiated cancer cells. Snu398 is the only cell line in which we detected FLT3 protein expression, suggesting that it is more aggressive than the others. Additionally, for the FLT3 signaling, FLT3 needs to bind its cognate ligand (FLT3L) to transduce signals and the expression of FLT3L in Snu398 was previously reported (24). Due to having expressions of FLT-3 and FLT3L, we chose Snu398 cells to explore the connection between FLT3 and HCC with in vitro and in vivo experimental approaches.

Tyrosine kinases are key cellular targets since their activation plays a critical role in increased cellular

proliferation and promotion of angiogenesis and metastasis (25,26). In fact, protein tyrosine kinase inhibitors have been heralded as a new kind of targeted therapy and are effective in treating a wide range of cancers (27). Thus, we performed in vitro cell proliferation, wound healing, and Matrigel invasion assays, and compared the results in the presence of kinase inhibitor K-252a or in the absence of FLT3. The cell proliferation assay was performed for 24 h in the case of K-252a treatment since this inhibitor may lose its effectiveness in a long culture period. However, we performed a cell proliferation assay for 72 h with shRNA transfected cells. Both inhibitor treatment and FLT3 knock-down resulted in a diminution in the proliferative capacity of Snu398 cells. The wound healing assay was done under both normal medium (10% FBS) and serum starvation (2% FBS) conditions. The reason for investigating the behavior of Snu398 cells under serum starvation condition was to block the proliferation of cells, allowing only the investigation of invasiveness of cells. Snu398 cells were treated with K-252a for 2 h after the wounds were generated. K-252a has been shown to inhibit kinase activity of FLT3 in a Ba/F3 cell line (28). There was an approximate twofold decrease in the invasive capacity of Snu398 cells following inhibitor treatment as compared with the untreated cells. This situation was observed under both normal and serum starvation conditions, confirming that these findings were not due to stalled proliferation, but to the invasiveness of Snu398 cells. Similar results were also obtained for the invasiveness of Snu398 cells when we knocked down the expression of FLT3 with specific FLT3 shRNA. Wound healing capacity of empty vector transfected cells was found to be higher as compared with the shRNA transfected ones under both normal medium and serum starvation conditions. As an additional approach to investigate further the effect of inhibitor treatment and knock-down, we performed a Matrigel invasion assay, and again there was a reduction in the invasive ability of inhibitor treated and shRNA transfected Snu398 cells as compared with that of the controls.

Our in vitro data suggest a role for FLT3 in the invasiveness of Snu398 cells. The in vitro effect of FLT3 has been shown to act through apoptosis in other cell types. It has been reported that FLT3 inhibition reduces Mcl-1 levels and induces Bax activation, resulting in mitochondrial apoptosis in acute myeloid leukemia (AML) cells (29). Furthermore, by using a selective FLT3 inhibitor, FI-700, they were able to enhance apoptosis in AML cells (30). In addition, targeting PDGF-receptor and FLT3 reduced survival and migration of human meningioma cells (31). Further studies are required to test whether the inhibition of FLT3 activity results in the disruption of apoptotic pathways in HCCs.

Inhibition of FLT3 with a different type III receptor tyrosine kinase inhibitor, MLN0518, has been shown to suppress tumor growth in mice bearing glioma xenografts (32). Another molecule, LY2801653, is an orally bioavailable multikinase inhibitor with potent activity against FLT3 and displays antitumor activities against colon, bile duct, and lung mouse xenograft models (33). In parallel, our results also showed that inhibiting the activity of FLT3 has an effect on HCC. The absence of tumors in the xenografts upon K-252a treatment provides strong evidence that the activity of FLT3 is required for tumor formation. It is tempting to speculate that FLT3 may also be a marker for cancer stem cells; however, this clearly requires new experiments to prove it. We have previously shown that the concentration of K-252a did not have any toxic effects (17). In addition, Snu398 cells were all viable prior to injection, and thus we were not concerned with K-252a's detrimental effects on cell viability.

In addition to FLT3's well known effect on cellular proliferation, FLT3 may also act by regulating the hypoxic tumor microenvironment. It is known that the microenvironment of the tumor has an important role in the pathogenesis and treatment of HCC since the hypoxic tumor microenvironment contributes greatly to the extent of tumorigenesis (34). The inhibition of the kinase activity of FLT3 by C-1311 potently reduced the transcription of the HIF-1-dependent reporter gene and the endogenous HIF-1 target gene, and showed anticancer activity (35). Therefore, it is tempting to speculate that inhibiting FLT3 either with shRNA or with specific inhibitors may reverse the effects of hypoxia in HCC and additional experiments are warranted to test this.

We also showed for the first time that the inhibition of the activity of FLT3 coincided with the reduction in αSMA positive cells in xenografts, suggesting FLT3's possible involvement during in vivo invasiveness. αSMA is a marker for epithelial mesenchymal transition (EMT), which has been shown to play a very important role in tumor invasiveness and normal developmental processes (36). The induction of EMT has been documented in the metastasis of many cancers, including HCC (37). Down-regulation of αSMA expressing cells after transfecting Snu398 cells with shRNA suggests a possible role for FLT3 during metastasis. However, the molecular mechanism of this effect remains to be resolved.

Finally, targeting a specific kinase instead of a group of kinases may also be useful in decreasing the side effects during therapy. One of the promising drugs currently used for advanced and intermediate HCC is sorafenib (Nexavar) (38). Sorafenib is a multikinase inhibitor with activity against RAF kinases and several receptor tyrosine kinases, including vascular endothelial growth factor receptor (VEGFR), platelet-derived growth factor receptor (PDGFR), FLT3, Ret, and c-Kit (39,40). Drug-related

adverse events in patients receiving sorafenib therapy include diarrhea and hand/foot skin reactions, and they may cause the discontinuation of treatment (41,42). The inhibition of VEGFR and PDGFR has been thought to be responsible for this effect (41,42). Therefore, to interfere only with the kinase activity of FLT3 may also be a useful approach to avoid the unwanted effects during therapy.

When all our findings are examined, a connection between FLT3 and HCC can be drawn. From the work described in this article we were able to show that the inhibition of FLT3 either by using an inhibitor for its kinase activity or after a stable knock-down with a specific shRNA, resulted in the diminution of proliferation, migration, and tumor forming abilities of HCCs both in vitro and in vivo. Therefore, in addition to acute myelogenous leukemia, FLT3 may also be a good therapeutic target in HCC treatment due to the impairment in tumor forming ability of HCC cells following the blockage of FLT3 activity.

Acknowledgments

The authors would like to thank Dr Yasemin Genç for statistical analysis and Drs Michelle Adams and Zeynep Tokcaer-Keskin for critical reading and editorial reviewing of the manuscript.

References

1. Jemal A, Bray F, Center MM, Ferlay J, Ward E, Forman D. Global cancer statistics. CA Cancer J Clin 2011; 61: 69–90.
2. Llovet JM, Burroughs A, Bruix J. Hepatocellular carcinoma. Lancet 2003; 362: 1907–1917.
3. Farazi PA, DePinho RA. Hepatocellular carcinoma pathogenesis: from genes to environment. Nat Rev Cancer 2006; 6: 674–687.
4. Matthews W, Jordan CT, Wiegand GW, Pardoll D, Lemischka IR. A receptor tyrosine kinase specific to hematopoietic stem and progenitor cell-enriched populations. Cell 1991; 65: 1143–1152.
5. Drexler HG, Quentmeier H. FLT3: receptor and ligand. Growth Factors 2004; 22: 71–73.
6. Piloto O, Wright M, Brown P, Kim KT, Levis M, Small D. Prolonged exposure to FLT3 inhibitors leads to resistance via activation of parallel signaling pathways. Blood 2007; 109: 1643–1652.
7. Stirewalt DL, Radich JP. The role of FLT3 in haematopoietic malignancies. Nat Rev Cancer 2003; 3: 650–665.
8. Matsusaka S, Tsujimura T, Toyosaka A, Nakasho K, Sugihara A, Okamoto E, Uematsu K, Terada N. Role of c-kit receptor tyrosine kinase in development of oval cells in the rat 2-acetylaminofluorene/partial hepatectomy model. Hepatology 1999; 29: 670–676.
9. Fausto N. Liver regeneration and repair: hepatocytes, progenitor cells, and stem cells. Hepatology 2004; 39: 1477–1487.
10. Aydin IT, Tokcaer Z, Dalgic A, Konu O, Akcali KC. Cloning and expression profile of FLT3 gene during progenitor cell-dependent liver regeneration. J Gastroenterol Hepatol 2007; 22: 2181–2188.
11. McGrath K, Palis J. Ontogeny of erythropoiesis in the mammalian embryo. Curr Top Dev Biol 2008; 82: 1–22.
12. Kinoshita T, Sekiguchi T, Xu MJ, Ito Y, Kamiya A, Tsuji K, Nakahata T, Miyajima A. Hepatic differentiation induced by oncostatin M attenuates fetal liver hematopoiesis. Proc Natl Acad Sci USA 1999; 96: 7265–7270.
13. Ozeki K, Kiyoi H, Hirose Y, Iwai M, Ninomiya M, Kodera Y, Miyawaki S, Kuriyama K, Shimazaki C, Akiyama H et al. Biologic and clinical significance of the FLT3 transcript level in acute myeloid leukemia. Blood 2004; 103: 1901–1908.
14. Zheng R, Levis M, Piloto O, Brown P, Baldwin BR, Gorin NC, Beran M, Zhu Z, Ludwig D, Hicklin D et al. FLT3 ligand causes autocrine signaling in acute myeloid leukemia cells. Blood 2004; 103: 267–274.
15. Isern J, Fraser ST, He Z, Baron MH. Developmental niches for embryonic erythroid cells. Blood Cells Mol Dis 2010; 44: 207–208.
16. Luc S, Buza-Vidas N, Jacobsen SE. Delineating the cellular pathways of hematopoietic lineage commitment. Semin Immunol 2008; 20: 213–220.
17. Bayin SN. The role of FLT3 in hepatocellular carcinogenesis. MSc, Bilkent University, Ankara, Turkey, 2010.
18. Bradford MM. A rapid and sensitive method for the quantification of microgram quantities of protein utilizing the principle of protein-dye binding. Anal Biochem 1976; 74: 248–254.
19. Yuzugullu H, Benhaj K, Ozturk N, Senturk S, Celik E, Toylu A, Tasdemir N, Yilmaz M, Erdal E, Akcali KC et al. Canonical Wnt signaling is antagonized by noncanonical Wnt5a in hepatocellular carcinoma cells. Mol Cancer 2009; 8: 90.
20. Petersen BE, Grossbard B, Hatch H, Pi L, Deng J, Scott EW. Mouse A6-positive hepatic oval cells also express several hematopoietic stem cell markers. Hepatology 2003; 37: 632–640.
21. Zhang Y, Bai XF, Huang CX. Hepatic stem cells: existence and origin. World J Gastroenterol 2003; 9: 201–204.
22. Joo SY, Choi BK, Kang MJ, Jung DY, Park KS, Park JB, Choi GS, Joh J, Kwon CH, Jung GO et al. Development of functional human immune system with the transplantations of human fetal liver/thymus tissues and expanded hematopoietic stem cells in RAG2-/-gamma(c)-/- MICE. Transplant Proc 2009; 41: 1885–1890.

23. Qiu C, Hanson E, Olivier E, Inada M, Kaufman DS, Gupta S, Bouhassira EE. Differentiation of human embryonic stem cells into hematopoietic cells by coculture with human fetal liver cells recapitulates the globin switch that occurs early in development. Exp Hematol 2005; 33: 1450–1458.

24. Krupp M, Itzel T, Maass T, Hildebrandt A, Galle PR, Teufel A. CellLineNavigator: a workbench for cancer cell line analysis. Nucleic Acids Res. 2013; 41: D942–D948.

25. Krause DS, Van Etten RA. Tyrosine kinases as targets for cancer therapy. N Engl J Med 2005; 353: 172–187.

26. Lemmon MA, Schlessinger J. Cell signaling by receptor tyrosine kinases. Cell 2010; 141: 1117–1134.

27. Arora A, Scholar EM. Role of tyrosine kinase inhibitors in cancer therapy. J Pharmacol Exp Ther 2005; 315: 971–979.

28. Cools J, Mentens N, Furet P, Fabbro D, Clark JJ, Griffin JD, Marynen P, Gilliland DG. Prediction of resistance to small molecule FLT3 inhibitors: implications for molecularly targeted therapy of acute leukemia. Cancer Res 2004; 64: 6385–6389.

29. Yoshimoto G, Miyamoto T, Jabbarzadeh-Tabrizi S, Iino T, Rocnik JL, Kikushige Y, Mori Y, Shima T, Iwasaki H, Takenaka K et al. FLT3-ITD up-regulates MCL-1 to promote survival of stem cells in acute myeloid leukemia via FLT3-ITD-specific STAT5 activation. Blood 2009; 114: 5034–5043.

30. Kojima K, Konopleva M, Tsao T, Andreeff M, Ishida H, Shiotsu Y, Jin L, Tabe Y, Nakakuma H. Selective FLT3 inhibitor FI-700 neutralizes Mcl-1 and enhances p53-mediated apoptosis in AML cells with activating mutations of FLT3 via Mcl-1/Noxa axis. Leukemia 2010; 24: 33–43.

31. Andrae N, Kirches E, Hartig R, Haase D, Keilhoff G, Kalinski T, Mawrin C. Sunitinib targets PDGF-receptor and FLT3 and reduces survival and migration of human meningioma cells. Eur J Cancer 2012; 48: 1831–1842.

32. Boult JK, Terkelsen J, Walker-Samuel S, Bradley DP, Robinson SP. A multi-parametric imaging investigation of the response of C6 glioma xenografts to MLN0518 (tandutinib) treatment. PLoS One 2013; 26: e63024.

33. Yan SB, Peek VL, Ajamie R, Buchanan SG, Graff JR, Heidler SA, Hui YH, Huss KL, Konicek BW, Manro JR et al. LY2801653 is an orally bioavailable multi-kinase inhibitor with potent activity against MET, MST1R, and other oncoproteins, and displays anti-tumor activities in mouse xenograft models. Invest New Drugs 2013; 31: 833–844.

34. Hernandez-Gea V, Toffanin S, Friedman SL, Llovet JM. Role of the microenvironment in the pathogenesis and treatment of hepatocellular carcinoma. Gastroenterology 2013; 144: 512–527.

35. Paradziej-Łukowicz J, Skwarska A, Peszyńska-Sularz G, Brillowska-Dabrowska A, Konopa J. Anticancer imidazoacridinone C-1311 inhibits hypoxia-inducible factor-1α (HIF-1α), vascular endothelial growth factor (VEGF) and angiogenesis. Cancer Biol Ther 2011; 12: 586–597.

36. Kalluri R, Weinberg RA. The basics of epithelial-mesenchymal transition. J Clin Invest 2009; 119: 1420–1428.

37. van Zijl F, Zulehner G, Petz M, Schneller D, Kornauth C, Hau M, Machat G, Grubinger M, Huber H, Mikulits W. Epithelial-mesenchymal transition in hepatocellular carcinoma. Future Oncol 2009; 5: 1169–1179.

38. Keating GM, Santoro A. Sorafenib: a review of its use in advanced hepatocellular carcinoma. Drugs 2009; 69: 223–240.

39. Ranieri G, Gadaleta-Caldarola G, Goffredo V, Patruno R, Mangia A, Rizzo A, Sciorsci RL, Gadaleta CD. Sorafenib (BAY 43-9006) in hepatocellular carcinoma patients: from discovery to clinical development. Curr Med Chem 2012; 19: 938–944.

40. Wilhelm SM, Adnane L, Newell P, Villanueva A, Llovet JM, Lynch M. Preclinical overview of sorafenib, a multikinase inhibitor that targets both Raf and VEGF and PDGF receptor tyrosine kinase signaling. Mol Cancer Ther 2008; 27: 3129–3140.

41. Autier J, Escudier B, Wechsler J, Spatz A, Robert C. Prospective study of the cutaneous adverse effects of sorafenib, a novel multikinase inhibitor. Arch Dermatol 2008; 144: 886–892.

42. Chu D, Lacouture ME, Fillos T, Wu S. Risk of hand-foot skin reaction with sorafenib: a systematic review and meta-analysis. Acta Oncol 2008; 47: 176–186.